Lab on a Chip

Micro- & nano- fluidic research for chemistry, physics, biology, & bioengineering

www.rsc.org/loc

Volume 11 | Number 5 | 7 March 2011 | Pages 761–980

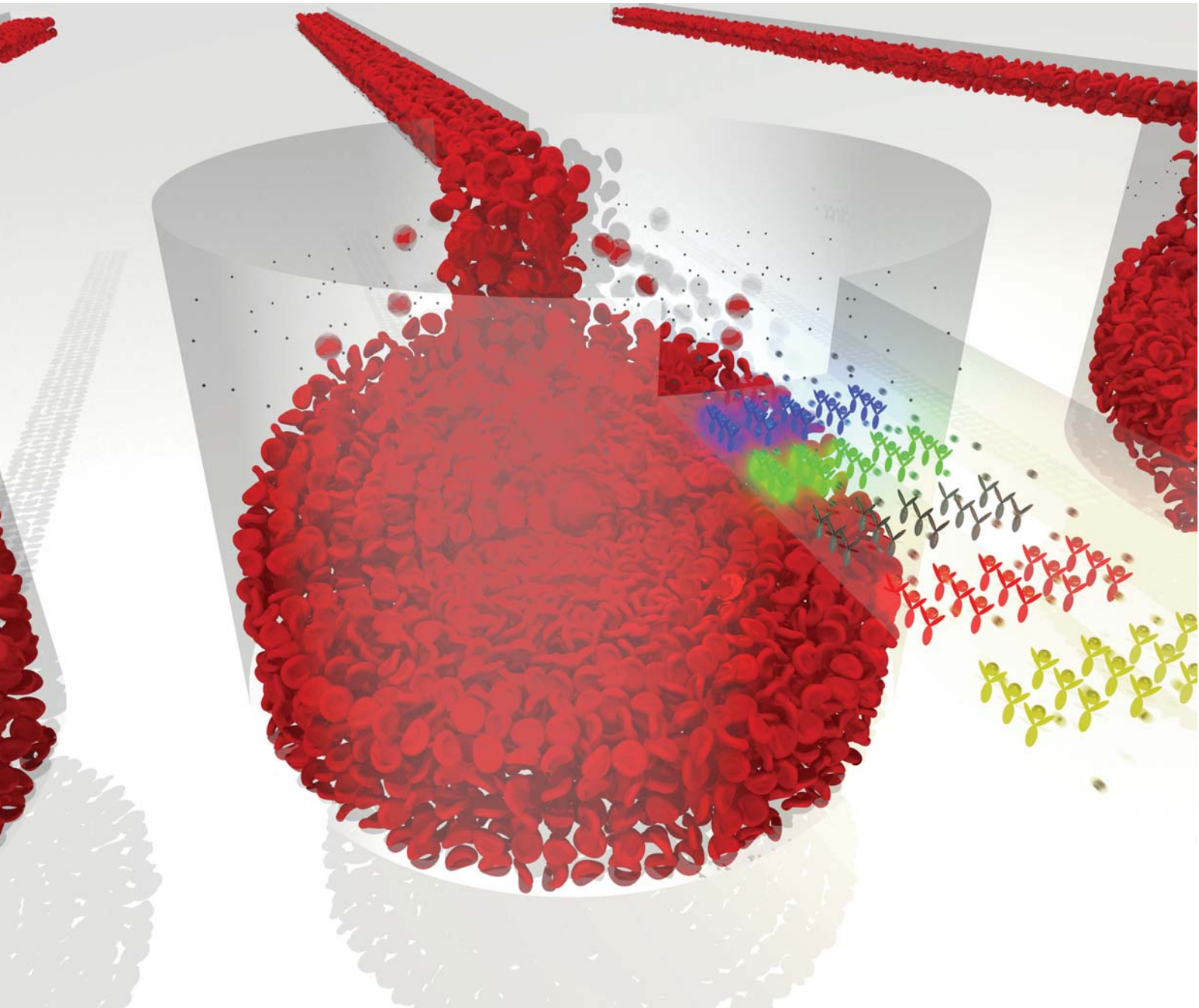

ISSN 1473-0197

RSC Publishing

PAPER

Lee *et al.*

Stand-alone self-powered integrated microfluidic blood analysis system (SIMBAS)

Stand-alone self-powered integrated microfluidic blood analysis system (SIMBAS)†

Ivan K. Dimov,‡[abc] Lourdes Basabe-Desmonts,‡[a] Jose L. Garcia-Cordero,‡[a] Benjamin M. Ross,[b] Antonio J. Ricco[a] and Luke P. Lee*[ab]

Received 12th September 2010, Accepted 19th October 2010
DOI: 10.1039/c0lc00403k

We present a self-powered integrated microfluidic blood analysis system (SIMBAS) that does not require any external connections, tethers, or tubing to deliver and analyze a raw whole-blood sample. SIMBAS only requires the user to place a 5 μL droplet of whole-blood at the inlet port of the device, whereupon the stand-alone SIMBAS performs on-chip removal of red and white cells, without external valving or pumping mechanisms, followed by analyte detection in platelet-containing plasma. Five complete biotin–streptavidin sample-to-answer assays are performed in 10 min; the limit of detection is 1.5 pM. Red and white blood cells are removed by trapping them in an integral trench structure. Simulations and experimental data show 99.9% to 100% blood cell retention in the passive structure. Powered by pre-evacuation of its PDMS substrate, SIMBAS' guiding design principle is the integration of the minimal number of components without sacrificing effectiveness in performing rapid complete bioassays, a critical step towards point-of-care molecular diagnostics.

Introduction

Blood is a treasure-trove of information about the functioning of the body, particularly at the molecular level.[1] At present, blood testing is mainly performed in centralized clinical laboratories, with blood tests accounting for most of the 740 tests performed in typical large clinical laboratories;[2] they represent an estimated annual cost of US$ 50 billion.[3]

Typical blood tests require several millilitres of blood sample and have relatively long analysis times (>1 h). Sample transportation requirements[4] add further variability to sample analysis time. Recent studies have found that the time between blood plasma separation and plasma analysis is critical for plasma proteome consistency.[5] Furthermore because most blood analyses are based on optical detection techniques, the separation of plasma from blood cells is often critical to decrease the interference of cells (primarily red cells) with the optical path, thereby increasing assay sensitivity and reliablity.

Microfluidic technology has demonstrated that laboratory instruments and assays can be miniaturized to a fraction of their size, leading to lower costs per measurement, shorter sample analysis times, less sample handling with its inherent errors, and better reproducibility in both basic research[6] and clinical[7] applications. For blood plasma analysis, microfluidic technology can miniaturize and simplify the analysis steps and eliminate the need for sample handling, transportation, and storage, which can potentially increase the quality, reproducibility, and reliability of the assay results.

Most microfluidic technologies for on-chip plasma separation require 'umbilical' tubes (or electrical wires in the case of electrokinetic approaches) for fluid delivery, propulsion, and control. They also require external pumping mechanisms (syringe pumps, compressed air, electro-pneumatic systems, high-voltage power supplies, or motors) making device control and operation more complex, cumbersome, and expensive. Separation of plasma on microfluidic devices has been demonstrated using different techniques and platforms, including employing microfilter-like parallel arrays of shallow channels,[8] exploiting the Zweifach-Fung effect,[9] and using the Lab-on-a-CD platform.[10]

To become useful diagnostics tools in point-of-care settings, microfluidic systems will require further improvement by integration of sample preparation with metering mechanisms, possibly including on-board reagent storage, incorporation of multiplexed biomarker detection on a single device, and minimization of the number of user steps required to perform an assay, all without compromising device functionality or assay sensitivity. Some of the most important improvements will include reducing the complexity of the microfluidic design and decreasing the amount of external support equipment required, while simultaneously reducing the number of on-chip components (such as valves), the number of fabrication steps, and the range of different materials used. These steps will decrease the cost of manufacture while increasing device reliability. A valid criticism of many current microfluidic systems aimed at the commercial market is that their high-volume manufacturing costs would be prohibitive.[11]

A case in point is the automated blood-analysis chip integrated with on-chip plasma separation that was recently demonstrated by Heath *et al.*[12] The micro-device was reported to have exquisite

[a]*Biomedical Diagnostics Institute, National Centre for Sensor Research, Dublin City University, Glasnevin, Dublin 9, Ireland; Fax: +353 1 7006558; Tel: +353 1 700 7658*
[b]*Biomolecular Nanotechnology Center, Berkeley Sensor and Actuator Center, Department of Bioengineering, University of California, Berkeley, CA, USA. E-mail: lplee@berkeley.edu; Tel: +1 510 642 5855*
[c]*Department of Biomedical Engineering, Universidad de Valparaíso, Valparaíso, Chile; Tel: +56 32 2686848*

† Electronic supplementary information (ESI) available: Supporting details; Fig. S1–S3; Movie SF1. See DOI: 10.1039/c0lc00403k

‡ These authors contributed equally.

limits of detection for multiple biomarkers. However, several external solenoid valves were needed for operation of on-chip valving and pumping. Plastic tubing was needed to deliver and move blood samples to the device. In an effort to make a self-contained, self-powered multiplexed protein assay chip, the same group developed a microfluidic H_2O_2-powered pressure pump that drives on-chip fluid flow.[13] This method was shown to be effective, but for the device to function requires loading and regulation of the H_2O_2 fuel, a tight seal during the operational steps, and the integration of electrodes.

A more practical method for implementing on-chip flow propulsion was proposed by Maeda *et al.*[14] and consists of exploiting the free volume of PDMS. Air (and water vapor) molecules are first evacuated from a PDMS substrate by placing it in a vacuum container for a period of time. Potential energy is stored by the evacuated bulk material until the device is brought into contact with atmospheric pressure, whereupon flow is generated in dead-end microchannels as the free volume of the PDMS refills with air and/or water vapor. This mechanism, which was applied to power an on-chip sequential injection immunoassay,[15] demonstrates that the properties of device substrates can be used to propel fluid into dead-end microchannels without the need for external pumps. Flow control is possible by adjusting the air-evacuation time or microchannel hydrodynamic resistance, and by creating porosity in the substrate.

We report here a two-step, self-contained and self-powered integrated microfluidic blood analysis system (SIMBAS) that integrates whole-blood plasma separation from red and white blood cells with multiple immunoassays. We harness the physical properties of PDMS in combination with the microfluidic channel resistance to propel fluid into and through the channels, so SIMBAS does not require any external support equipment other than an optical detection system. SIMBAS utilizes two-step operation: after removing the device from its vacuum pouch or container, the user simply dispenses the sample droplets onto the multiple inlets of the device for multiple blood sample analyses and then reads the results in a fluorescent scanner. The number of fabrication steps has been minimized to 4 (see ESI† for details) and the fabricated microfluidics are monolithic, enhancing considerably the potential for low-cost, high-volume manufacture.

The SIMBAS concept (Fig. 1) aims to minimize the number of components while achieving the stand-alone, untethered single-chip integration required to perform assays that meet the challenging requirements of point-of-care diagnostics. Specifically, SIMBAS integrates sample volume metering, plasma separation from whole human blood, multiple immuno-assays, and flow propulsion into a robust (monolithic), fast (10 min. to result), portable, low-cost, low-sample-volume (5 μL), simple-to-use (two user steps) disposable platform with the potential to enable novel global-health diagnostic applications.

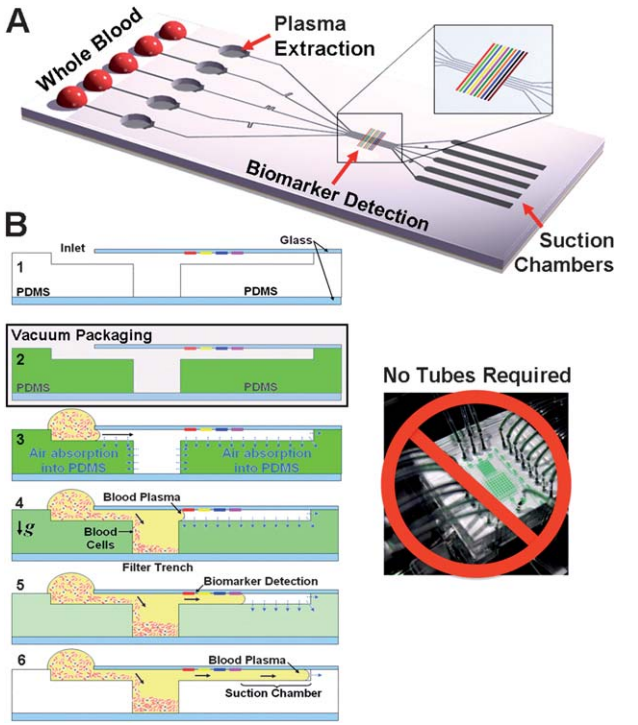

Fig. 1 Self-priming, self-contained, tether-free SIMBAS (A) integrates (i) volume metering (ii) plasma separation from whole-blood (iii) multiple biomarker detection and (iv) suction chambers for fluid propulsion. (B) Cross section of device operation: (2) storage in low pressure, *e.g.* vacuum package; (3) within 2 min of removing the device from vacuum conditions and placing a 5 μL whole-blood sample on the inlet, degas-driven flow propels the sample into the device; (4) as the whole-blood passes over the filter trench, blood cells sediment gravitationally and are filtered while plasma flows into the channel; (5) plasma-based proteins are detected as the plasma flows across the biomarker detection zone; (6) suction chamber regulates the total volume of plasma analyzed and stops the flow before the trench filters are overfilled.

Experimental

Fabrication of SIMBAS

The device was fabricated by placing a 2 mm thick PDMS layer between two glass microscope slides (VWR International Inc., USA); see ESI† for fabrication details. The 2 mm thick PDMS layer contains the microfluidic channels and the filtering trenches.

The microfluidic channels face the top slide. The bottom slide serves as a support layer as well as a bottom seal to the filter trench. To prevent blood cells from flowing past the filter trench, the top slide was manually coated with a hydrophobic pen (PAP Hydrophobic Barrier Pen for Immunochemistry, Abcam, UK) only on the region that overlaps the filter trenches.

Protein patterning

Prior to assembling the device, the bio-recognition site on the top glass slide was patterned by microcontact printing[16] to create 15 μm wide lines of avidin (Sigma Aldrich, USA). The deposited lines were perpendicular to the flow direction. See ESI† for fabrication and patterning protocol. Patterned substrates were used typically on the day of preparation.

Blood collection and sample preparation

Whole-blood samples were collected from finger pricks using a capillary blood collection system (Minicollect Tube LH

Lithium Heparin; 1 mm safety lancet; capillary for heparin 250 μL from Greiner Bio-One U.K.) according to the manufacturer's instructions. Blood samples were used on the microdevice within 20 min of drawing from patients.

ATTO557-Biotin (Sigma Aldrich, USA) in PBS was spiked in the whole-blood samples at different concentrations (1.5 μM to 1.5 pM).

Device activation and operation

The SIMBAS device is activated by maintaining it in a low-pressure (<0.3 atm) condition for at least 15 min. The low-pressure condition can be achieved either by placing the device in a standard vacuum desiccator (Sigma Aldrich, U.K.) at ~200 Torr. To perform an assay, the user simply removes the device from the low-pressure environment and then loads the whole-blood sample onto the inlets of the device. No further steps are required by the user. In the current implementation, sample loading has to be done within 2 min of removing the SIMBAS from the low-pressure environment.

Approximately 5 μL of whole-blood collected directly from a finger prick is sufficient for a complete assay. The assay is finished when the blood plasma fills the suction chamber and reaches the end channel. For these initial laboratory demonstrations, readout is accomplished by detaching the PDMS slab from the upper glass slide (see ESI† Fig. S2) to permit its readout in a fluorescent scanner (ScanArray GX PLUS Microarray Scanner, Perkin Elmer, USA). Fluorescent intensities of the images were analysed using ImageJ software.

Filter trench characterization

Three different trench diameters, 1 mm, 2 mm, and 3 mm, were tested as follows: the devices were fixed in place on a light microscope (Nikon, USA) with a CCD camera (QImaging Go-5, Canada); the lighting and focus remained fixed during the course of an experiment. Defibrinated sheep blood (Hemostat, USA) was flowed through the device, and the flow rate was controlled using a syringe pump (Pump 11, Harvard Apparatus, USA). The flow rate was varied from approximately 2 μL h^{-1} to 400 μL h^{-1} while images were captured at each flow rate. The maximum speed for each device was determined by the filling of the trench with blood cells, and for the maximum speeds tested, the trenches filled with blood cells in a few tens of seconds and the devices ceased to operate effectively. Therefore, a smaller trench diameter requires a lower maximum speed. Additionally, the hematocrit content of the blood (H_t) was artificially altered from its initial value of 37%. To achieve a lower hematocrit content of 17.5%, the blood was diluted in phosphate-buffered saline (PBS, Gibco, Invitrogen, Carlsbad, CA). For higher hematocrit content, blood was spun in a centrifuge to separate the blood cells from plasma, plasma was removed to achieve a hematocrit of 74%, and the blood cells were re-suspended using gentle mixing. For each flow rate, at least 3 images were recorded to determine mean and standard deviation values for the cell capture efficiency.

To determine the cell-capture efficiency of each device, the images at each flow rate were analyzed using a custom Matlab script. Data were analyzed as follows: a region of interest (ROI) was manually identified for each experiment at the outlet of the trench, and the intensities of the ROI pixels were considered. For each pixel in the ROI, the percent capture efficiency at a given flow rate was determined by:

$$\eta_{pixel} = 100 \cdot [1 - (V - V_i)/(V_f - V_i)] \quad (1)$$

where V is the intensity value for that pixel at the flow rate, V_i is the intensity of the same pixel when the device is in its initial state (no flow), and V_f if the average intensity of the same pixel when the trench has been filled and whole-blood is flowing through the ROI. The overall efficiency of the device was computed by averaging the efficiency values of all pixels in the ROI.

Simulation settings

To model the filter trench capture efficiency, the forces on a cell or particle suspended within a fluid as it passes over the trench must be accounted for; see ESI† Fig. S3A. The relevant forces are the buoyancy-corrected gravitational sedimentation force $\mathbf{F_{gb}}$ and the fluid drag force $\mathbf{F_d}$.

$$\mathbf{F_{gb}} = \Delta m_p \mathbf{g} \quad (2)$$

where Δm_p represents the difference in the masses of the particle and the displaced fluid volume and $\mathbf{g}$ the gravitational acceleration. Thus, particle trajectories can be calculated by solving the force balance equation for any given particle:

$$m_p \frac{d^2\mathbf{r}}{dt^2} = \mathbf{F_d}\left(t, \mathbf{r}, \frac{d\mathbf{r}}{dt}\right) + \mathbf{F_{gb}} \quad (3)$$

where t represents time and $\mathbf{r}$ the position vector of the particle. The fluid drag force is modeled by the Khan and Richardson force,[17] an empirical estimation of the fluid drag force on spherical particles that is valid for a wide range of Reynolds numbers (including Re < 1):

$$|\mathbf{F_d}| = \pi {r_p}^2 \rho (|\mathbf{v} - \mathbf{v}_p|)^2 \left[1.84 \mathrm{Re}_p^{-0.31} + 0.293 \mathrm{Re}_p^{0.06}\right]^{3.45}$$
$$\mathrm{Re}_p = \frac{(|\mathbf{v} - \mathbf{v}_p| 2 r_p \rho)}{\eta} \quad (4)$$

where the suspended spherical particle has a mass m_p a radius r_p and a particle velocity $\mathbf{v}_p$ immersed in a fluid with a density ρ, dynamic viscosity η, and a velocity $\mathbf{v}$. Eqn (3) and (4) were used in combination with the Navier–Stokes equations to calculate the particle trajectories and therefore estimate the trench capture efficiency (see ESI† for simulation settings).

Results and discussion

SIMBAS principle

In its current format, SIMBAS can analyze up to 5 whole-blood samples concurrently using 5 equivalent-length units. Each unit consists of three operating sections. Firstly, the self-powered plasma separation section is composed of a round filter trench (~2 mm diameter and ~2 mm deep) for capturing (through sedimentation) and filtering out the red and white blood cells from whole-blood. Secondly, the multiple-biomarker detection region is composed of sample channel (~80 μm high, 50 μm wide, and 10 mm long) with immobilized specific-capture protein bars

(in this case 15 μm wide streptavidin bars). Finally, the integrated suction chambers (with dead end channels) regulate the assay volume.

SIMBAS does not require any external pumping, propulsion or control mechanisms; instead, it stores potential energy directly in its high-gas-solubility polymeric substrate material (in this case, PDMS). Flow within the device is generated by degassing ("activating") the chip in a low-pressure environment within a standard vacuum desiccator or a low-pressure package;[14] see Fig. 2. When a 5-μL whole-blood sample is placed within 2 min of removing the SIMBAS from the low-pressure environment in such a way that the blood sample completely seals the inlet, the potential energy of the evacuated PDMS drives absorption of air in the dead-end micro-channel, reducing the internal pressure in the channel (if its open end is occluded, *e.g.* by a liquid sample). This generates a pressure difference that draws whole-blood into the device.

Control of flow rate

The flow rate can be controlled though several parameters including the degassing time t_d (the time the device is stored in low pressure) and idling time t_i (defined as the time from the ventilation of the low pressure to sample introduction).

Hosokawa *et al.*[14] showed that if t_i is kept below 5 min, the flow rates will be maximum and reproducible. In the case of a 100 μm × 25 μm × 9 mm channel, flow rates of 0.5–2 nL min^{-1} were readily achieved.[14] The degassing time used by Hosokawa *et al.*[14] was 1–3 h. In order to reduce the long times and shorten the experimental setup time, we characterized the effect of a lower t_d (5–20 min) on the device filling rate. A t_d as low as 15 min can generate enough degas-driven flow to completely fill the device in 8 min (see ESI† Fig. S1).

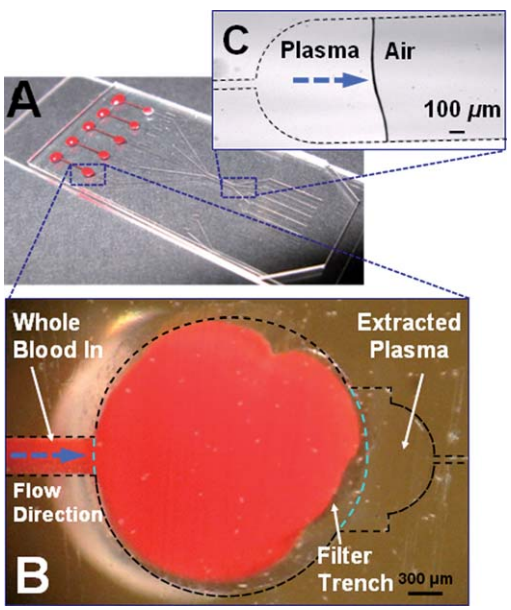

Fig. 2 Degas-driven flow is generated when the SIMBAS device is removed from a low-pressure environment. (A) Fast and effective plasma separation of 5 separate whole-blood samples by (B) filter trench (cylindrical cavity) and gravity-driven blood cell sedimentation generates blood-cell-free plasma in the self-priming untethered SIMBAS, see ESI† Movie SF1. (C) Plasma fills the suction chamber.

Maximizing capture efficiency of blood cells in trench

Blood cells are approximately 10% more dense than the plasma in which they are suspended.[18] For more than 100 years[19] it has been known that blood under the influence of gravity sediments and separates into its fundamental components (plasma, white blood cells, red blood cells). On the conventional macro-scale, however, this process requires hours. Miniaturizing this process into a microfluidic system reduces the sedimentation and separation time to several minutes: the cells are effectively separated over much shorter length scales. For the separation to function, the residence times of white and red cells within the trench should allow them to sediment below the 80 μm deep flow channels and remain effectively captured within the trench. The residence time can be controlled by the size of the trench and the flow rate across the top of the trench.

To maximise the trench filter efficiency, we began by investigating the effect of the trench design parameters (depth, length, and flow rate) on the cell capture efficiency. The simulation results (Fig. 3) indicate that as long as the length and depth of the trench, normalized to the height of the inlet channel, exceed 5, and the velocity is no greater than 90 μm s^{-1}, the capture efficiency should be ~100%.

Based on these results, filter trench dimensions were chosen: $L = 2$ mm, $h_1 = 2$ mm, and $h_0 = 80$ μm. This results in a normalised length and depth of 25. To experimentally verify trench filter efficiency, several trench lengths (*i.e.* diameters) were tested. As the trench length is enlarged, the flow rate over the trench diminishes and the cell sedimentation depth increases. We investigated the filter efficiency of trenches with lengths ranging from 1 to 3 mm. The results, shown in Fig. 4, indicate ~100% capture efficiency for all trenches at flow rates below 50 μL h^{-1}. It was also observed that the larger the trench, the higher the flow rate that can be sustained while still capturing ~100% of blood cells. For a trench diameter of 3 mm, it is possible to flow blood at rates close to 1 mL h^{-1} while maintaining high capture efficiency. Furthermore, blood with low or high hematocrit H_t levels (18.5% and 74%, respectively) can also be filtered with very high efficiency. The flow rate can be increased by an order of magnitude by increasing the trench diameter (0.05 mL h^{-1} for a 1 mm diameter and 1 mL h^{-1} for a 3 mm diameter).

No blood cells were observed in the separated plasma (Fig. 2C); however, since platelets sediment at much lower rates, they are observed in the extracted plasma (data not shown).

It is important to note that this separation method relies only on sedimentation and not cross flow; thus, there is no need for a precisely-manufactured μm-scale gap or any other size-exclusion filtration mechanism of the sort that has been extensively reported in the literature.[8] This greatly reduces fabrication (and, ultimately, manufacturing) complexity and increases the robustness of the system, particularly to clogging. In addition, the design is very forgiving of flow rate instability, making it compatible with degas-driven flow.

The SIMBAS sedimentation-based system separates plasma from whole-blood without diluting the sample, which is critical for the detection of low-abundance proteins. Generally,

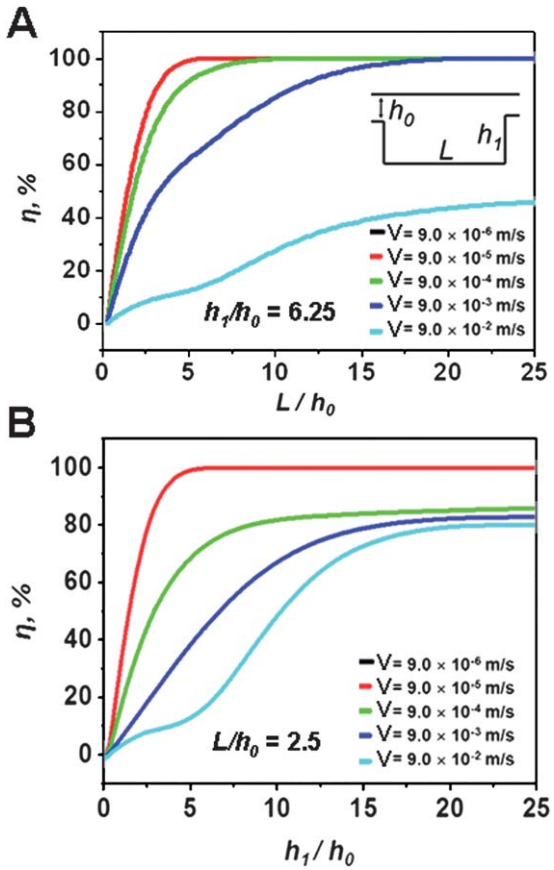

Fig. 3 The computed effects of trench geometry and blood flow rate on filtration efficiency. (A) Effects of trench length normalized to inlet channel height (L/h_0), as well as inlet velocity (V), on particle capture efficiency, η. (B) Effects of trench depth normalized to inlet channel height (h_1/h_0), along with inlet velocity (V), on particle capture efficiency. As shown in the inset L is the length of the trench, h_1 its depth, and h_0 the height of the inlet channel. Note that as the normalized length and depth of the trench increase, capture efficiency improves; as the inlet velocity decreases, capture efficiency also increases. Simulations with inlet velocity $V = 9.0 \times 10^{-6}$ and $V = 9.0 \times 10^{-5}$ produced identical capture efficiencies, thus the results overlap and the $V = 9.0 \times 10^{-6}$ is not visible.

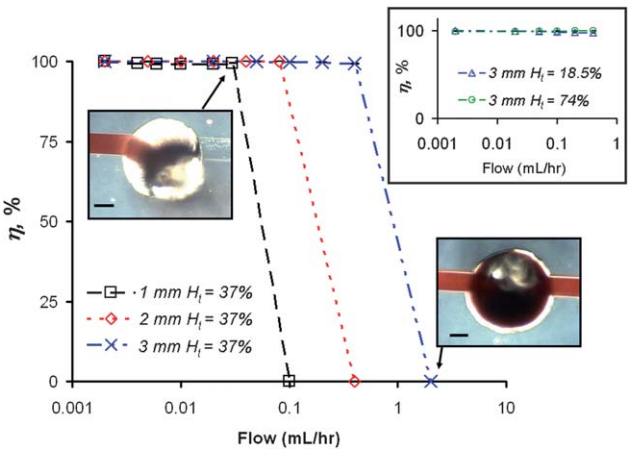

Fig. 4 Characterization of blood cell trench filtration efficiency η for multiple flow rates and trench lengths. Inset shows η for extreme hematocrit levels (H_t). The empirical data suggest that as long as the flow rate is kept below 50 μL h^{-1}, ~100% filtration efficiency can be achieved. Note all measured points have a standard deviation less than 0.2% (n = 3). Scale bars are 500 μm.

cross-flow systems such the one described by Tachi *et al.*[20] dilute the extracted sample because they require buffer flow to minimize clogging at the cross-flow filtration barrier.

In contrast to cross-flow and many other sedimentation-based approaches, SIMBAS is fully functional during chip priming (the initial fluid filling and bubble elimination): it does not need pre-priming to initiate the flow conditions used for separation (see ESI† Movie SF1). Importantly, this feature eliminates user preparation steps and makes SIMBAS an easy-to-use two-step system appropriate for challenging health-care settings.

Integration of plasma separation with analyte detection

After plasma separation, the sample is directed to the biomarker detection site where specific capture proteins are immobilized on the channel ceiling (Fig. 1B). A glass substrate is used as the channel ceiling, allowing use of well-developed glass-based immobilization chemistries. 15 μm wide streptavidin bars were patterned using microcontact printing and physisorption. Beyond the detection region are the integrated suction chambers, the purpose of which is to regulate the total volume of sample flow through the biomarker detection site.

Because this is a closed system, *i.e.*, inlets but no outlets, the total fluid volume can be controlled by choosing the volumes of the suction chambers (dead-end channels). Once the suction chambers are completely filled, the flow stops across the entire chip. The flow over the trench also ceases and thus cells already captured in the trench remain there, without overflowing into the biomarker recognition area.

Analyte detection was demonstrated using a streptavidin–biotin binding assay (Fig. 5). To avoid non-specific protein responses, whole-blood samples were spiked with various concentrations of fluorescently-labeled biotin. Fluorescent readout was performed by disassembling the device and inserting the top glass slide into a standard microarray scanner (one way to read this device in many current clinical settings). The results of the self-contained SIMBAS show that within 10 min 1.5 pM biotin can be readily detected in whole-blood (Fig. 5B). Note that the 1.5 pM signal is significantly above the background, so by further optimizing the probe surface attachment and the channel depth, the level of detection can be significantly improved. For clinically relevant biomarkers, antibody–antigen on-rates could be much lower and the equilibrium dissociation rates higher compared to the streptavidin–biotin binding pair used in this study. One way to compensate for lower sensitivity could be to increase the perfused sample volume and augment the concentration of the binding sites. This can be accomplished by changing the suction chamber volume and the binding site surface area.

The sample-to-sample assay reproducibility was measured by spiking three whole-blood samples with 150 pM biotin. This resulted in an approximate standard error of 13.6% (inset, Fig. 5B).

Another important advantage of SIMBAS is that it does not require irreversible bonding between the PDMS and glass layers,

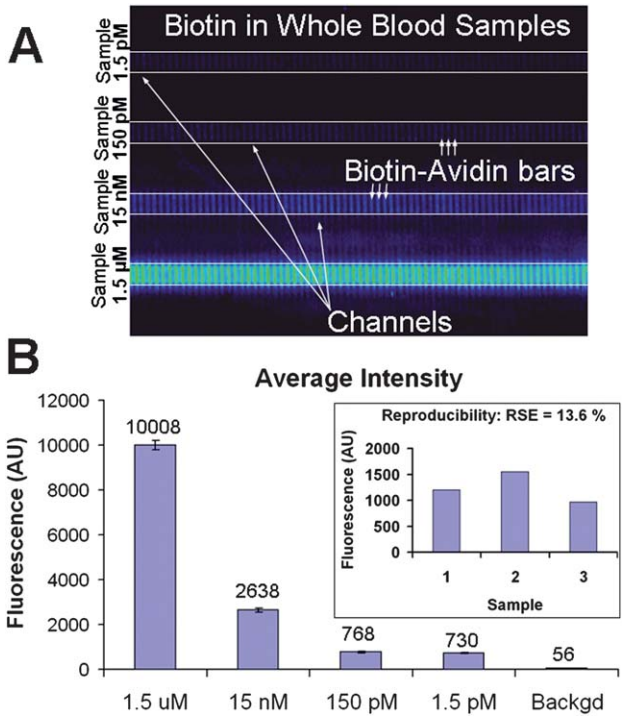

Fig. 5 Detection of fluorescently-labeled biotin in whole-blood samples using stand-alone SIMBAS. (A) Fluorescent readout of the biomarker detection sites of four different samples. Each channel has a different sample with a different concentration of biotin. (B) Levels of detection of biotin in whole-blood. Inset: Sample-to-sample reproducibility at 150 pM; note that the inset data were obtained with a different optical gain from the limit-of-detection measurements.

so it can be easily disassembled, allowing the glass layer with the captured analytes to be used for further analysis (ESI† Fig. S2 shows the disassembly schematic). For multi-analyte detection, each streptavidin bar (Fig. 3A) can be replaced with a different probe, such as mono- or poly-clonal antibodies. In the case where multiple probe chemistries are not compatible under the same conditions, the design allows fluidic isolation of each category of probes (as demonstrated by the separate samples) into separate channels in order to minimize negative interferences. In this way, each SIMBAS would allow the detection of several thousand biomarkers or analytes from a few micro-litres of sample.

For mass production, the SIMBAS device could be manufactured in part from thermoplastic by substituting the glass substrate with a rigid polymer substrate, with appropriate changes in surface functionalization chemistries. A thermoplastic material with sufficiently rapid air permeability and significant free volume, potentially abetted by addition of porosity, might also be used instead of PDMS, substantially reducing the manufacturing complexity and cost by the use of a single thermoplastic resin for the entire device. For commercialisation purposes a vacumm sealed packing (see ESI† Fig. S1A) may be used to keep the device "activated" and ready for use as well as to ensure good long term storage conditions for the onboard bio-recognition reagents.

Conclusions

In summary, we have demonstrated a self-contained, tether-free SIMBAS that very efficiently extracts blood plasma from less than 5 μL of whole-blood and performs multiple protein binding assays with high sensitivity without any external pumping mechanisms. This sample-to-answer monolithic device could be manufactured at low cost (based on polymer injection molding). Our integrated device is well-suited for point-of-care applications because of its self-powering mechanism, disposability, and simplicity of use and two-step operation. Furthermore, the device allows for direct blood analysis without delay (in 10 min) or sample manipulation, which should reduce the likelihood of sample contamination, increase result reproducibility and quality, and help eliminate errors due to sample handling and labeling mistakes. For point-of-care diagnostics, the logical design of SIMBAS with minimal need for component integration is critical for maximum effectiveness in performing bioassays.

Acknowledgements

The authors acknowledge the Science Foundation Ireland (Grant No. 05/CE3/B754) and National Institutes of Health (R01CA120003) for financial support of the project.

References

1 M. Toner and D. Irimia, *Annu. Rev. Biomed. Eng.*, 2005, **7**, 77–103.
2 T. M. Bailey, American Clinical Laboratory, 1997.
3 MedPro Month, *Diagnostic testing, outcomes and POC*, Vol. VII: (No. 1), Medical Data International, January 1997.
4 I. R. Lauks, *Acc. Chem. Res.*, 1998, **31**, 317–324.
5 H. Sen-Yung, C. Ren-Kung, P. Yi-Hsin and L. Hai-Lun, *Proteomics*, 2006, **6**, 3189–3198.
6 K. S. Samuel and M. W. George, *Electrophoresis*, 2003, **24**, 3563–3576.
7 S. Nagrath, L. V. Sequist, S. Maheswaran, D. W. Bell, D. Irimia, L. Ulkus, M. R. Smith, E. L. Kwak, S. Digumarthy, A. Muzikansky, P. Ryan, U. J. Balis, R. G. Tompkins, D. A. Haber and M. Toner, *Nature*, 2007, **450**, 1235–1239.
8 S. Yang, A. Undar and J. D. Zahn, *Lab Chip*, 2006, **6**, 871–880.
9 V. VanDelinder and A. Groisman, *Anal. Chem.*, 2006, **78**, 3765–3771.
10 S. Haeberle, T. Brenner, R. Zengerle and J. Ducree, *Lab Chip*, 2006, **6**, 776–781.
11 J. L. Garcia-Cordero, D. Kurzbuch, F. Benito-Lopez, D. Diamond, L. P. Lee and A. J. Ricco, *Lab Chip*, 2010, **10**, 2680–2687.
12 R. Fan, O. Vermesh, A. Srivastava, B. K. H. Yen, L. Qin, H. Ahmad, G. A. Kwong, C.-C. Liu, J. Gould, L. Hood and J. R. Heath, *Nat. Biotechnol.*, 2008, **26**, 1373–1378.
13 L. Qin, O. Vermesh, Q. Shi and J. R. Heath, *Lab Chip*, 2009, **9**, 2016–2020.
14 K. Hosokawa, K. Sato, N. Ichikawa and M. Maeda, *Lab Chip*, 2004, **4**, 181–185.
15 K. Hosokawa, M. Omata, K. Sato and M. Maeda, *Lab Chip*, 2006, **6**, 236–241.
16 A. Bernard, J. P. Renault, B. Michel, H. R. Bosshard and E. Delamarche, *Adv. Mater.*, 2000, **12**, 1067–1070.
17 J. M. Coulson and J. F. Richardson, *Particle Technology and Separation Processes*, 5 edn, Pergamon, Oxford, 1991.
18 E. Ponder, *J. Biol. Chem.*, 1942, 333–338.
19 E. Biernacki, *Gazeta Lekarska*, 1897, **17**, 962, 996.
20 T. Tachi, N. Kaji, M. Tokeshi and Y. Baba, *Anal. Chem.*, 2009, **81**, 3194–3198.

Supplementary Material (ESI) for Lab on a Chip

Support Information

Self-Contained, Self-Powered Integrated Microfluidic Blood Analysis System (SIMBAS)

Ivan K. Dimov, Lourdes Basabe-Desmonts, Jose L. García-Cordero, Benjamin M. Ross, Antonio J. Ricco and Luke P. Lee

Fabrication of SIMBAS

The microfluidic channels were fabricated using standard soft lithography replica molding techniques[13]. Briefly, a mould was created through a single-layer process using negative photoresist, SU8-2100 (Microchem U.S.A.), which was spun onto a clean silicon wafer using a spin-coater (P6700 Specialty Coating Systems, Inc., U.S.A.) to form an 80-µm thick layer. The photoresist was poured onto the wafer at 500 rpm; the angular speed was then ramped up to 2500 rpm for 30 sec with an acceleration of 300 rpm/s. Next, the wafer was soft-baked at 65 ºC for 5 min and 95 ºC for 30 min, followed by UV-exposure for 10 s at 9.5 mW/cm^2 using a mask aligner (Karl-Süss KSM MJB-55W). The wafer was then baked for 5 min at 65 ºC and 12 min at 95 ºC, and allowed to cool to room temperature. Finally, the wafer was developed in SU8 developer (Microposit EC Solvent, Chestech Ltd., UK) for 4 min, rinsed with isopropanol, and blown dry using N_2.

PDMS (Sylgard 184, Dow Corning) was prepared with a 10:1 mass ratio (base to cross-linker); degassed in a vacuum chamber for 30 min; then poured on the SU8 mold to a thickness of ~ 2mm; then cured in an oven at 60 ºC for at least 10 h. The PDMS was then carefully peeled off the mould. The PDMS was punched with a 2-mm outer-diameter flat-tip needle (Technical Innovations, Inc, Texas, USA) to form the circular filter trenches. Up to 5 trenches were punched in one chip. The PDMS fluidic layer was placed in conformal contact with the glass slides, providing reversible sealing.

Considering that the microfluidic mould is produce once and is sufficient for making multiple chips, the production of a single SIMBAS chip requires 4 steps:

1. Casting and curing the PDMS on the microfluidic mould.
2. Peeling, and punching the filter trenches.
3. Protein pattering of the bio-recognition site on the upper glass slide.
4. Placing the PDMS fluidic layer in conformal contact with the upper and lower glass slides.

Fabrication of PDMS stamps for microcontact printing

Prior to assembling the device, the bio-recognition site on the top glass slide was patterned by microcontact printing[13] to create 15-µm-wide stripes of avidin (Sigma Aldrich, U.S.A.) Patterned PDMS stamps were fabricated by pouring a 10:1 (v/v) mixture of Sylgard 184 elastomer and curing agent over a patterned silicon master. Fabrication of the patterned silicon master was done as follows: MICROPOSIT™ S1818™ Positive Photoresist was spun at 5500 rpm for 30 sec on a silicon wafer. The coated wafer was then cured for 1 min on a vacuum hot plate at 115 °C. UV light irradiated the photoresist layer for 20 sec through a photomask (Photronics, Mid Glamorgan, South Wales, UK). Resultant features were developed by dipping the master in developer MF319 (Chestech Ltd, Warwickshire, UK) for 40 sec; finally, it was rinsed with water and dried under nitrogen. Subsequently, masters were exposed to a vapor of (tridecafluoro-1,1,2,2-tetrahydrooctyl)-1-trichlorosilane (Sigma Aldrich Inc., Ireland) under vacuum for 1 h to facilitate the release of the PDMS mold after curing.

The mixture was cured for one hour in an oven at 60 ºC, then carefully peeled away from the master and left in the oven for another 18 h at 60 ºC to ensure complete curing. Prior to inking, the stamps were oxidized by exposure to UV/ozone for 10 min. This process causes the stamp surface to become hydrophilic, which ensures homogeneous spreading of the ink (*i.e.*, the protein solution). The stamps were freshly prepared no more than two days prior to use.

Protein-Patterned Surfaces

Standard microscope slides were used as glass substrates for the protein patterning. The slides were rinsed with ethanol and N_2 dried. The PDMS stamps were ozone-activated and immediately inked with 50 µL of a 200 µg/mL Neutravidin (a deglycosylated version of avidin, Sigma Aldrich, U.S.A) solution in phosphate-buffered saline (PBS) for at least 15 min. Excess ink solution was removed from the PDMS surface with a pipette and the stamp was then blown dry with nitrogen. The stamp was brought into contact with the glass substrate for 5 min. After protein micropatterning, the glass slides were immersed in BSA solution (10 mg/mL) in PBS, blocking any uncovered regions of the glass surface, for at least 1 h at room

temperature. The slides were rinsed with PBS and water, and then N_2 dried prior to assembling the device and using it for blood analysis. Typically, patterned substrates were used on the same day as their preparation.

Flow rate characterisation

Flow rates were characterised by loading the device with 10 μM 7-dichlorofluorescein (DCF) green fluorescent dye dissolved in Milipore pure water (Millipore, U.S.A.). The loaded device was placed on an IX80 (Olympus, Japan) inverted fluorescence microscope and irradiated for 100 ms every 40 sec with a 492-nm excitation beam (excitation filter BP492/18 with a xenon light source, CellR MT20, Olympus); 530-nm fluorescent light was sampled through a filter cube (U-MF2, Olympus) with a CCD sensor (Hamamatsu C4742-80-12AG). The images were analysed with the CellR software package to reveal the kinetics of the channel filling.

Simulations

The flow patterns were calculated by means of the two-dimensional Navier-Stokes equations for total continuity, energy, and momentum.

$$0 = \nabla u \tag{1}$$

$$\rho \frac{\partial u}{\partial t} + \rho u \cdot \nabla u = \nabla \cdot [-\rho I + \eta \nabla u] + F \tag{2}$$

where u is the velocity of the flowing mixture, ρ is the fluid density, I is the inertia force, μ is the dynamic viscosity, and F is the external body force.

To estimate blood cell (*i.e.* particle) trapping efficiency in the micro-trench system, the Kahn and Richardson force for particle trajectory was calculated. In order to accurately explain the process dynamics, this work focused on the effects of the geometrical parameters, flow velocity, and particle trapping efficiency (see Table 1). The pressure boundary condition was used for the inlet and the outlet. In the computational analysis, 50 particles were tracked, and estimated boundary conditions were used, as listed in Table 2. The trench simulation was performed in a two-dimensional triangular grid consisting of 1,168 cells using commercial computational fluid dynamics (CFD) software, COMSOL ver 3.4 and CFD-ACE. The semi-implicit pressure-linked equation (SIMPLE) algorithm was applied to solve the momentum equation. The calculation for each case took about 5 min of run time on an Intel Xeon E5420 @ 2.50 GHz.

Table 1. Flow and device parameters

Parameter	Values
Relative* trench height h_1/h_0	0.25, 2.5, 6.25, 12.5, 25
Relative* trench length L/h_0	0.25, 2.5, 6.25, 12.5, 25
Fluid and particle velocity (m/s)	9.0×10^{-2}, 1.8×10^{-3}, 9.0×10^{-3}, 9.0×10^{-4}, 9.0×10^{-5}
Particle diameter, D_p/h_0	2.5×10^{-1}
Particle density (kg/m^3)	1.1×10^3

*relative to inlet channel height, h_0

Table 2. Boundary conditions

Boundary	Condition	Value
Inlet	Pressure boundary, P_{in}	0.04, 0.4, 4, 20, 40 Pa
Outlet	Pressure boundary, P_{out}	0
Wall	No slip	-

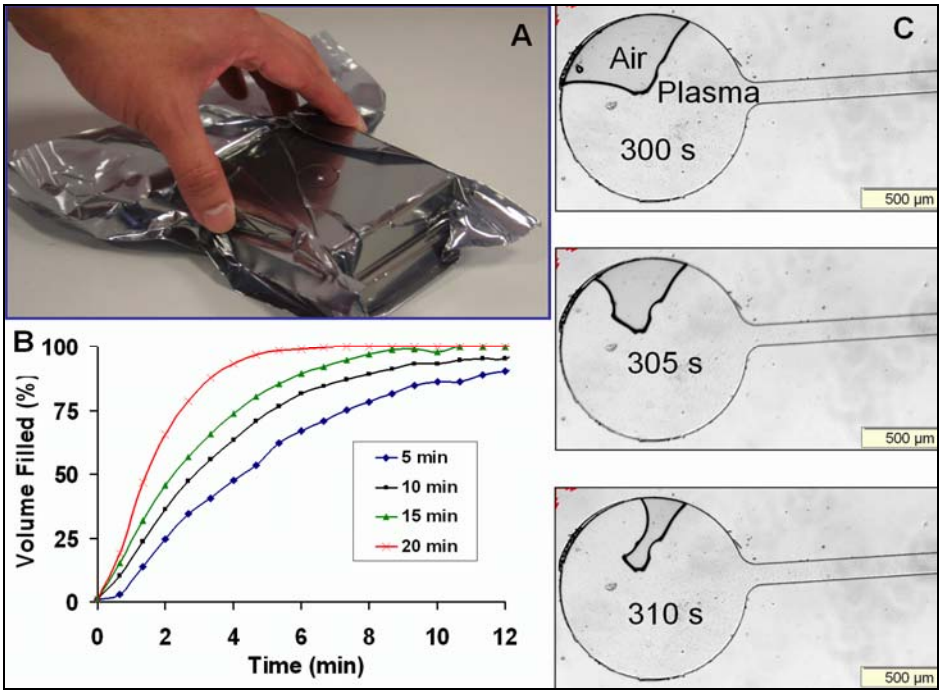

Fig. S1 (A) Degas-driven flow is generated when the SIMBAS device is removed from a low-pressure environment and a fluid sample introduced. (B) Different degassing times t_d were tested (5 min to 20 min) for generating degas-driven flow into dead-end channels made of PDMS. (C) Monitoring the filling process after degassing the PDMS device in a standard vacuum desiccator.

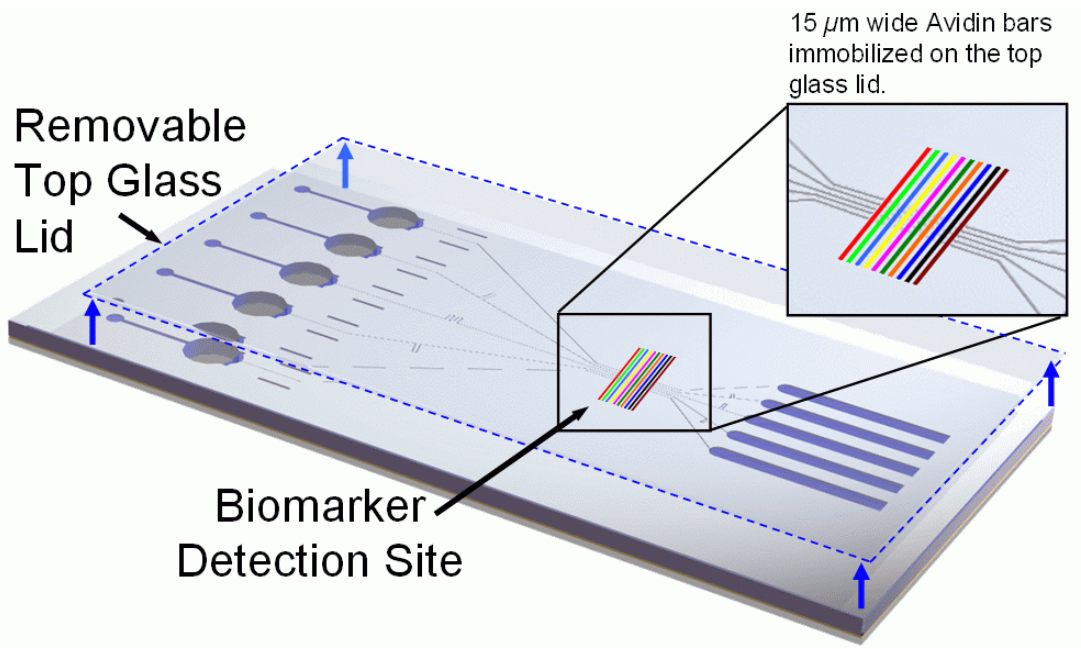

Fig. S2 Analytes from the biomarker detection matrix can be accessed for further analysis such as PCR, CE, MS, etc. by disassembling the chips after the assay: only reversible PDMS-glass bonding is used.

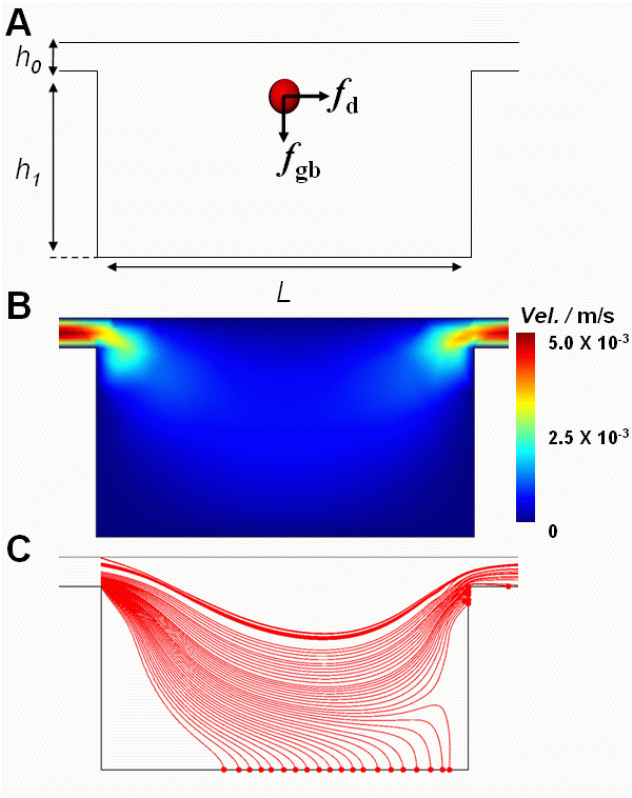

Fig. S3 Modelling and simulation of particle capture by the SIMBAS microfluidic trench system. (A) The principal forces acting on a blood cell or suspended particle within the trench are the buoyancy-corrected gravitational sedimentation force f_{gb} and the fluid drag force f_d. (B) Fluid velocity field within the microfluidic trench system as calculated by the two-dimensional Navier-Stokes equations for total continuity, energy, and momentum. (C) Particle trajectory traces for multiple particles with variable initial positions. Most particles are captured or filtered out, but a few of those that start near the top of the inlet channel escape to the outlet.